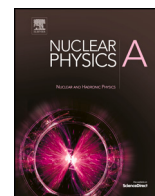


Contents lists available at [ScienceDirect](https://www.sciencedirect.com)

## Nuclear Physics A

journal homepage: [www.elsevier.com/locate/nuclphysa](http://www.elsevier.com/locate/nuclphysa)

# Coupled channels and production of near-threshold $B^{(*)}\bar{B}^{(*)}$ resonances in $e^+e^-$ annihilation

S.G. Salnikov<sup>a,b,\*</sup>, A.E. Bondar<sup>a,b</sup>, A.I. Milstein<sup>a,b</sup><sup>a</sup> Budker Institute of Nuclear Physics, 630090, Novosibirsk, Russia<sup>b</sup> Novosibirsk State University, 630090, Novosibirsk, Russia

## ARTICLE INFO

## Keywords:

Final state interaction

Hadron production

 $B$  mesons

## ABSTRACT

The effects of final-state interaction of hadrons, produced in  $e^+e^-$  annihilation near the threshold, are discussed. If there is a loosely bound state or a virtual state in a system of produced hadrons, then the energy dependence of hadroproduction cross section is very strong. Our approach is based on the use of the effective potentials accounting for the interaction between hadrons in the final state. The cases of a few channels with nonzero transition amplitudes between them are considered. It is shown that these transitions drastically change the energy dependence of the cross sections. In particular, a narrow resonance below the threshold in one channel leads to a broad peak in another channel. We explained the non-trivial energy dependence of the production cross sections of  $B\bar{B}$ ,  $B^*\bar{B}$ ,  $B\bar{B}^*$ ,  $B^*\bar{B}^*$  near the thresholds in  $e^+e^-$  annihilation and obtained good agreement between our predictions and the experimental data available.

## 1. Introduction

Typical values of potentials, describing interaction of hadrons, are relatively large (hundreds of MeV), and the radii of these potentials are about 1 fm. Therefore, a loosely bound state may exist with the modulus of binding energy much less than a depth of the potential well. In this case, the scattering length  $\xi$  is positive and considerably exceeds the radius  $a$  of the potential. The binding energy  $\varepsilon$  is expressed via the scattering length as  $\varepsilon = -1/M\xi^2$ , where  $M$  is the mass of hadrons. It is also possible that there is no bound state, but a slight increase in the potential depth leads to appearance of such a state (so-called virtual state). In this case the scattering length is negative, and its absolute value is much larger than  $a$ . The energy of the virtual state is defined as  $\varepsilon = 1/M\xi^2$ . In both cases (bound or virtual state) a resonance is observed in the hadron scattering cross section.

The process of heavy meson or baryon production in  $e^+e^-$  annihilation starts with heavy quark-antiquark pair production at small distances of the order of  $1/\sqrt{s}$ . At larger distances the final state consists of mesons or baryons described by the wave function  $\psi(r)$ . Therefore, the production cross section of heavy hadrons is proportional to  $|\psi(0)|^2$  for a pair in the s-wave,  $|\psi'(0)|^2$  for a pair in the p-wave, etc. (see Refs. [1,2]). Here  $\psi(0)$  is the wave function at distances  $r \ll a$  and  $r \gg 1/\Lambda_{QCD}$ . The latter condition allows one to consider the produced hadronic state in terms of mesons and baryons but not in terms of quarks and antiquarks. Note that  $\psi(0)$  is nothing but the inverse of the Jost function (see, f.i., [3]).

For a low-energy bound or virtual state, the absolute value of the wave function or its derivative inside the potential well is much larger than the corresponding values in the absence of interaction potential. As a result, the hadroproduction cross sections increase

\* Corresponding author.

E-mail addresses: [S.G.Salnikov@inp.nsk.su](mailto:S.G.Salnikov@inp.nsk.su) (S.G. Salnikov), [A.E.Bondar@inp.nsk.su](mailto:A.E.Bondar@inp.nsk.su) (A.E. Bondar), [A.I.Milstein@inp.nsk.su](mailto:A.I.Milstein@inp.nsk.su) (A.I. Milstein).<https://doi.org/10.1016/j.nuclphysa.2023.122764>

Received 28 August 2023; Received in revised form 15 September 2023; Accepted 19 September 2023

Available online 22 September 2023

0375-9474/© 2023 Elsevier B.V. All rights reserved.

near the thresholds of the corresponding processes. Note that the shape of near-threshold resonances differs drastically from that obtained using the commonly used Breit-Wigner formula.

At present, near-threshold resonances in  $e^+e^-$  annihilation have been observed in many processes:  $e^+e^- \rightarrow p\bar{p}$  [4–11],  $e^+e^- \rightarrow n\bar{n}$  [12–14],  $e^+e^- \rightarrow \Lambda\bar{\Lambda}$  [15–18],  $e^+e^- \rightarrow \Lambda_c\bar{\Lambda}_c$  [19,20],  $e^+e^- \rightarrow B\bar{B}$  [21], and others. In all these cases, the shapes of near-threshold resonances differ from that described by the Breit-Wigner formula and differ also from each other. The shapes of resonances are determined by many factors: isotopic structure of the produced states, angular momentum, magnitude of tensor forces, the Coulomb interaction of charged particles, and others. For instance, tensor forces are responsible for transitions between the states with different angular momenta and affect the ratio of hadron electromagnetic form factors. The account for the final-state interaction of produced hadrons allows one to describe all experimental data within the same approach (see Refs. [22–29] and references therein).

In addition to a non-trivial behavior of the hadroproduction cross sections near the corresponding thresholds, the production cross sections of light mesons reveal a strong energy dependence near the same thresholds. This behavior is due to production of virtual hadrons below and above threshold with subsequent annihilation into light mesons. Examples of such processes are  $e^+e^- \rightarrow 6\pi$  [9,30–32],  $e^+e^- \rightarrow K^+K^-\pi^+\pi^-$  [9,33,34],  $J/\psi \rightarrow \gamma\eta'\pi^+\pi^-$  [35], and others. The unusual energy dependence of the cross sections of these processes has been explained by the interaction of virtual hadrons in the intermediate state [28,36,37].

In this work, we use the final-state interaction approach to describe the production of  $B\bar{B}$ ,  $B\bar{B}^*$ ,  $B^*\bar{B}$ ,  $B^*\bar{B}^*$  in  $e^+e^-$  annihilation near the thresholds of these processes. The corresponding experimental data are published in Refs. [21,38–40]. In Refs. [25,41], the final-state interaction approach was used to study the effects of isotopic invariance violation in the production of  $B\bar{B}$  and  $B^*\bar{B}^*$  near the thresholds. Since the states  $B\bar{B}$ ,  $B\bar{B}^*$ ,  $B^*\bar{B}^*$ , produced in  $e^+e^-$  annihilation, have identical quantum numbers  $J^{PC} = 1^{--}$ , then the amplitudes of transitions between these states are not zero. These transitions are irrelevant to the effects of isotopic invariance violation, since only narrow region close to the peak of resonance is essential. However, the account for the transition amplitudes is crucial for the description of the entire energy region near the thresholds of coupled channels. This is the main goal of our paper.

The paper is organized as follows. In Section 2, using a simple potential model of rectangular wells, we elucidate the main features of the resonance production cross sections near the thresholds in the cases of one channel, two channels, and three channels. In Section 3, our approach is applied to description of the experimental data on the cross sections of  $B^{(*)}\bar{B}^{(*)}$  pair production near the thresholds. The main results obtained are summarized in Conclusion.

## 2. Simple model

In this section, using a simple approach, we discuss the cross sections of  $e^+e^-$  annihilation into hadron-antihadron pairs near the thresholds of the processes. This approach allows one to understand the origin of the enhancement of the cross sections and to achieve good agreement with available experimental data as well. We consider the cases of one, two, and three channels in the final state having the same quantum numbers  $J^{PC}$  and close thresholds. We show that the shape of the cross section drastically depends on the number of channels due to transitions between them.

### 2.1. One channel

Let us consider only one channel when the radial wave function  $\psi(r)$  of produced hadrons satisfies the Schrödinger equation

$$\left( p_r^2 + MV + \frac{l(l+1)}{r^2} - k^2 \right) \psi(r) = 0, \quad (1)$$

where  $(-p_r^2)$  is the radial part of the Laplacian operator,  $M$  is the hadron mass,  $k = \sqrt{ME}$ ,  $E$  is the kinetic energy of a pair counted from the reaction threshold, and  $V$  is the interaction potential. We are interested in regular solution  $\psi_R(r)$  with asymptotic behavior

$$\psi_R(r \rightarrow \infty) = \frac{1}{2ikr} (S\chi^+ - \chi^-), \quad \chi^\pm = \exp[\pm i(kr - \pi l/2)]. \quad (2)$$

Cross section of pair production in the state with angular momentum  $l$  is given by the relation (see, e.g., Refs. [25,28] and references therein)

$$\sigma = \frac{2\pi\beta\alpha^2}{s} \left| g \psi_R^{(l)}(0) \right|^2, \quad (3)$$

where  $\beta = k/M$  is the hadron velocity,  $s = (2M + E)^2$ , and  $\psi_R^{(l)}(r) = (\partial/\partial r)^l \psi_R(r)$ . The coefficient  $g$  is related to the amplitude of pair production at small distances  $\sim 1/\sqrt{s}$  and can be considered as an energy independent constant.

The strong energy dependence of the cross section near the threshold appears if there is a bound state with a small value of binding energy or a low-energy virtual state. In the latter case a small increase of the potential depth leads to appearance of a bound state with a small binding energy. To illustrate this point, let us consider a rectangular potential well  $V(r) = U\theta(a-r)$ , where  $U < 0$ , and  $\theta(x)$  is the Heaviside function. For  $l = 0$ , Eq. (1) can easily be solved analytically. As a result, the wave function at the origin reads

$$\psi_R(0) = \frac{q e^{-ika}}{q \cos(qa) - ik \sin(qa)}, \quad q = \sqrt{M(E-U)}. \quad (4)$$

Near the threshold, we have  $k \ll q$ . Then, the cross section (3) is enhanced if

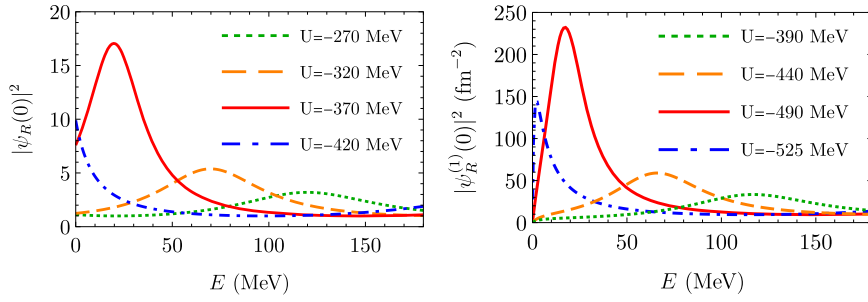


Fig. 1. The energy dependence of  $|\psi_R(0)|^2$  for  $l=0$  (left) and  $|\psi_R^{(1)}(0)|^2$  for  $l=1$  (right). The radius  $a = 1.5$  fm and a few values of  $U$  are used.

$$q_0 a \approx \pi \left( n + \frac{1}{2} \right) + \delta, \quad |\delta| \ll 1, \quad (5)$$

where  $q_0 = \sqrt{M|U|}$ , and  $n$  is an integer. Under this condition a low-energy bound or virtual state exists in the potential well. For  $|\delta| \ll 1$ , the scattering length is  $\xi = 1/q_0 \delta$ , where  $\delta > 0$  for the bound state with the binding energy  $\varepsilon = -1/M\xi^2$ , and  $\delta < 0$  for the virtual state with the energy  $\varepsilon = 1/M\xi^2$ . In both cases  $|\varepsilon| \ll |U|$ .

By means of Eqs. (4) and (5) the expression for  $|\psi_R(0)|^2$  can be simplified (see Ref. [29]):

$$|\psi_R(0)|^2 = \frac{q^2}{q^2 \cos^2(qa) + k^2 \sin^2(qa)} \approx \frac{\gamma |U|}{(E + \varepsilon_0)^2 + \gamma E},$$

$$\gamma = 4\kappa^2 |U|, \quad \varepsilon_0 = 2\kappa \delta |U|, \quad \kappa = \frac{1}{\pi(n + 1/2)}. \quad (6)$$

Corresponding energy dependence of the cross section (3) is equivalent to the Flatté formula [42], which is expressed in terms of the scattering length and the effective range of interaction. Note that for the rectangular potential well the latter equals to the radius  $a$  of the potential. One can easily verify that the precise and approximate formulas for the cross section are in good agreement with each other for  $|\delta| \ll 1$  and  $E \lesssim \varepsilon_0 \ll |U|$ . Note that  $|\varepsilon_0| \gg |\varepsilon|$  for both bound and virtual states, namely  $\varepsilon_0 \approx 2|\varepsilon|\xi/a$ . However, the position of peak in the cross section, which is proportional to  $\sqrt{E}|\psi_R(0)|^2$ , is located at energy  $E \approx |\varepsilon|$  for both bound and virtual states.

Thus, the description of near-threshold resonances by means of Flatté formula or by model potential is equivalent. However, the approach based on the use of model potential significantly simplifies consideration in the case of multiple coupled channels. The effective potential method is very convenient for account of the Coulomb interaction between hadrons. It is especially powerful for calculation of the total cross section of a process which includes an annihilation of real or virtual hadron pairs into light mesons, see, e.g., Ref. [28] and references therein.

We emphasize that model potentials can have significantly different shapes, but at the same time give close values of the scattering length and effective range of interaction, so that the shapes of the resonances will also be similar. Therefore, to describe near-threshold resonances it is convenient to use the simplest form of effective potentials. This is the approach we use in our work, choosing potentials in the form of rectangular wells, the parameters of which follow from comparing the predictions of the model with the experimental data.

As an example, we set  $M = M_B$ , where the mass of neutral  $B$  meson is  $M_B = 5279.65$  MeV. The energy dependence of  $|\psi_R(0)|^2$  with the wave function given in Eq. (4) is shown in Fig. 1 for  $a = 1.5$  fm and a few values of potential well depths. For such value of  $a$ , the bound state with  $n = 3$  appears at  $U = -396$  MeV. At  $U = -420$  MeV there is a bound state with binding energy  $\varepsilon = -12$  MeV. For  $U = -370$  MeV, there is a virtual state, which results in the peak in the energy dependence of  $|\psi_R(0)|^2$  at  $E \approx 20$  MeV. For smaller values of the potential well depth, the peak becomes less pronounced.

For  $l = 1$ , the cross section of hadron production (3) is proportional to the factor  $|\psi_R^{(1)}(0)|^2$ . The analytical form of this quantity is given in Eq. (8) of Ref. [25]. The energy dependence of  $|\psi_R^{(1)}(0)|^2$  for  $a = 1.5$  fm and a few potential well depths is shown in Fig. 1. For  $l = 1$  and  $U = -504$  MeV, a loosely bound state, corresponding to  $n = 4$ , appears. At  $U = -525$  MeV there is a low-energy bound state with  $\varepsilon = -4$  MeV. For  $U = -490$  MeV, there is a virtual state, which leads to a peak in  $|\psi_R(0)|^2$  at  $E \approx 20$  MeV. As for  $l = 0$ , for smaller values of  $|U|$ , the peak becomes less lower and wider. Qualitatively, the pictures for  $l = 0$  and  $l = 1$  look very similar. Therefore, existence of a loosely bound state or a virtual state is possible for any angular momentum  $l$ , although the specific positions of resonances and their widths depend on  $l$ .

The energy dependence of the cross section within our simple model is shown in Fig. 2 for a few values of the potential parameters. We consider the cases when a low-energy bound or virtual state with  $l = 0$  or  $l = 1$  exists. It is seen that for some depth of the potential well there is a near-threshold peak in the cross section. As mentioned above, the position of this peak is determined by the energy of the virtual state, while the shape of this peak depends also on the effective range of interaction. The near-threshold peaks turned out to be quite smooth and the next peaks in the cross section are located much higher in energy.

Let us include into consideration the possibility for produced hadron pair to annihilate into other particles. The number of different final states in this inelastic process can be huge and the probability of such annihilation can be significant. Inelastic processes are

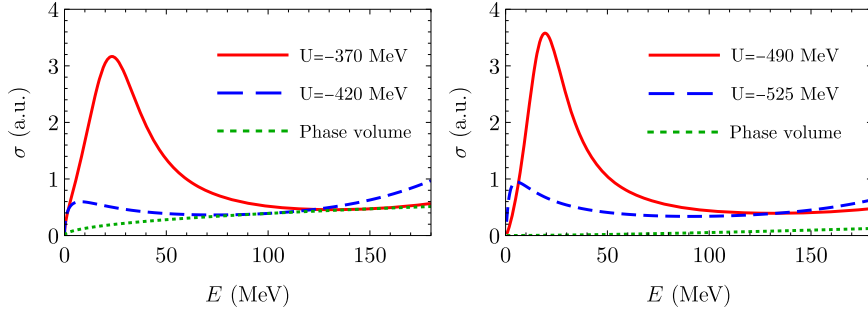


Fig. 2. The cross section of hadron pair production for  $l=0$  (left) and  $l=1$  (right) at  $a=1.5$  fm and various depths of the potential well. The cross section without final-state interaction corresponds to the energy dependence of the phase volume.

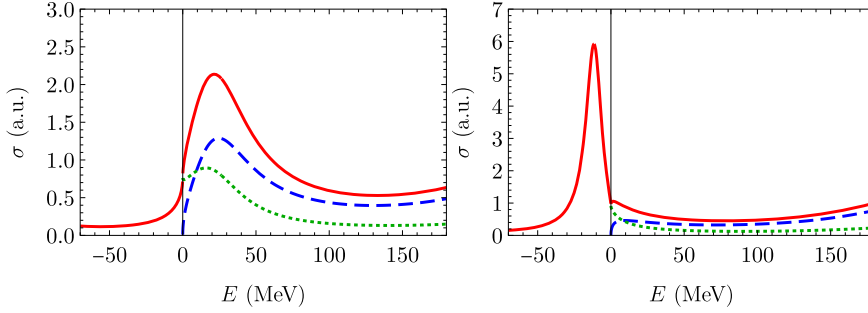


Fig. 3. The cross sections of hadron pair production for  $l=0$  and  $a=1.5$  fm. The depths of the optical potential are  $U = (-370 - 10i)$  MeV (left) and  $U = (-420 - 10i)$  MeV (right). The dashed line corresponds to  $\sigma_{el}$ , the dotted line to  $\sigma_{in}$ , and the solid line to  $\sigma_{tot}$ .

usually taken into account by means of so-called optical potentials in the same way as it is done in nuclear physics. These optical potentials contain not only the real part, but also the imaginary part. We refer to the cross section of real pair production as the elastic cross section,  $\sigma_{el}$ , which is given by Eq. (3). The inelastic cross section,  $\sigma_{in}$ , corresponds to the process, in which a produced virtual hadron pair annihilates into the final state. Note that the inelastic cross section, as well as the total cross section  $\sigma_{tot} = \sigma_{el} + \sigma_{in}$ , reveals a strong energy dependence near the threshold of real hadron pair production. This effect was discovered experimentally (see, e.g., Refs. [9,30–34]) and then have been explained theoretically (see Ref. [28] and references therein).

The total cross section is expressed via the Green's function  $D(r, r' | E)$  of the Schrödinger equation (see Ref. [28] and references therein):

$$\sigma_{tot} = \frac{2\pi\alpha^2}{Ms} |g|^2 \text{Im} D(0, 0 | E), \quad (7)$$

where  $D(r, r' | E)$  satisfies the equation

$$\left( p_r^2 + MV + \frac{l(l+1)}{r^2} - k^2 \right) D(r, r' | E) = \frac{1}{rr'} \delta(r - r'). \quad (8)$$

The Green's function can be expressed in terms of the regular solution  $\psi_R(r)$  and the non-regular solution  $\psi_N(r)$  of Eq. (1), having the asymptotics

$$\psi_N(r \rightarrow \infty) = \frac{1}{kr} \chi^+. \quad (9)$$

We have

$$D(r, r' | E) = k (\psi_R(r)\psi_N(r')\theta(r' - r) + \psi_R(r')\psi_N(r)\theta(r - r')). \quad (10)$$

For  $l=0$  one can easily obtain the analytical expression for the imaginary part of the Green's function

$$\text{Im} D(0, 0 | E) = \text{Im} \left[ q \frac{q \sin(qa) + ik \cos(qa)}{q \cos(qa) - ik \sin(qa)} \right]. \quad (11)$$

Note that for complex potential  $U$  the quantity  $q$  is also complex. For  $\text{Im} U = 0$ , the cross section  $\sigma_{tot}$  above the threshold coincides with the elastic cross section  $\sigma_{el}$ . Below the threshold  $\sigma_{tot}$  contains contributions of possible bound states. For energy  $E < 0$ , the momentum  $k$  should be considered as having positive imaginary part, namely  $k = \sqrt{M(-|E| + i0)}$ .

The energy dependence of the cross sections  $\sigma_{el}$ ,  $\sigma_{in}$  and  $\sigma_{tot}$  is shown in Fig. 3 for  $\text{Im} U = -10$  MeV. The left and right plots correspond, respectively, to the cases when a virtual state and a bound state exist. Though the imaginary part of potential is small,

the elastic cross section is significantly smaller than that for  $\text{Im} U = 0$  (cf. Fig. 2). At the same time, above the threshold the inelastic cross section  $\sigma_{\text{in}}$  becomes comparable to  $\sigma_{\text{el}}$ . Below the threshold, a peak is observed if a bound state exists. The width and height of this peak are determined by the imaginary part of the optical potential. With vanishing of the imaginary part of the potential, this peak turns into a  $\delta$ -function at the energy of a bound state. Naturally, in the case of a virtual level, a peak below the threshold does not occur.

## 2.2. Two channels

Let us consider now a two-channel process in which hadron pairs appear with the same quantum numbers  $J^{PC} = 1^{--}$ , close masses but different spins. To be specific, we will talk about pairs in the states  $X = B\bar{B}$  and  $Y = (B^*\bar{B} - B\bar{B}^*)/\sqrt{2}$ . Since the spins of  $B$  and  $B^*$  mesons are different, the interaction potential  $V_{XX}$  between  $B$  and  $\bar{B}$  differs slightly from the interaction potential  $V_{YY}$  between  $B^*$  and  $\bar{B}$ . In addition, identical quantum numbers  $J^{PC}$  make transition between the  $X$  and  $Y$  states to be possible. The corresponding off-diagonal matrix element  $V_{XY}$  is small compared to the potentials  $V_{XX}$  and  $V_{YY}$ . However, the value of  $V_{XY}$  should be compared not with these potentials, but with the energies of the real or virtual states. We show that in this case the energy dependence of the pair production cross sections differs noticeably from the case of  $V_{XY} = 0$ .

In the near-threshold energy region the wave function of produced hadron pairs satisfies the coupled-channel Schrödinger equation

$$\left( p_r^2 + M_B \mathcal{V} + \frac{l(l+1)}{r^2} - \mathcal{K}^2 \right) \Psi(r) = 0, \quad \mathcal{K}^2 = \begin{pmatrix} k_X^2 & 0 \\ 0 & k_Y^2 \end{pmatrix}, \quad \mathcal{V} = \begin{pmatrix} V_{XX} & V_{XY} \\ V_{XY} & V_{YY} \end{pmatrix}. \quad (12)$$

Here  $k_X = \sqrt{M_B E}$ ,  $k_Y = \sqrt{M_B (E - \Delta)}$ ,  $\Delta = M_{B^*} - M_B = 45.97 \text{ MeV}$ ,  $M_B = 5279.65 \text{ MeV}$  and  $M_{B^*} = 5325.62 \text{ MeV}$  are the masses of corresponding neutral mesons. In Eq. (12), the wave function  $\Psi = (u, v)^T$  consists of a radial wave function  $u$  of the  $X$  state and the radial wave function  $v$  of the  $Y$  state. The superscript  $T$  denotes the transposition. In following, we assume that the angular momentum of pairs is  $l = 1$ , since it corresponds to the process of  $B$ -meson pair production in  $e^+e^-$  annihilation.

The cross sections of meson production in the case of two channels are

$$\begin{aligned} \sigma_X &= \frac{2\pi\beta_X\alpha^2}{s} \left| g_X u_{1R}^{(1)}(0) + g_Y v_{1R}^{(1)}(0) \right|^2, \\ \sigma_Y &= \frac{2\pi\beta_Y\alpha^2}{s} \left| g_X u_{2R}^{(1)}(0) + g_Y v_{2R}^{(1)}(0) \right|^2, \end{aligned} \quad (13)$$

where  $\beta_X = k_X/M_B$ , and  $\beta_Y = k_Y/M_B$ . Here  $u_{1R}$ ,  $v_{1R}$ ,  $u_{2R}$ , and  $v_{2R}$  are the corresponding components of the regular solutions  $\Psi_{1R}$  and  $\Psi_{2R}$  of Eq. (12). These solutions have the asymptotic forms at  $r \rightarrow \infty$

$$\begin{aligned} \Psi_{1R} &= \frac{1}{2ik_X r} (S_{11}\chi_X^+ - \chi_X^-, S_{12}\chi_Y^+)^T, \\ \Psi_{2R} &= \frac{1}{2ik_Y r} (S_{21}\chi_X^+, S_{22}\chi_Y^+ - \chi_Y^-)^T, \\ \chi_X^\pm &= \exp[\pm i(k_X r - \pi/2)], \quad \chi_Y^\pm = \exp[\pm i(k_Y r - \pi/2)]. \end{aligned} \quad (14)$$

Complex coefficients  $g_X$  and  $g_Y$  are related to the amplitudes of corresponding meson pair production at small distances, and  $S_{ij}$  are some constants.

In order to demonstrate how the interaction between channels affect the energy dependence of the cross sections, let us consider a few examples. We choose the parametrization of the potential in the form of rectangular wells with the same radius but different depths:

$$\mathcal{V} = \begin{pmatrix} U_{XX} & U_{XY} \\ U_{XY} & U_{YY} \end{pmatrix} \theta(a - r), \quad (15)$$

where the matrix elements  $U_{ij}$  and the radius  $a$  are some constants. Below we present the numerical results of our investigations within such a model. Let us first consider the values of  $U_{ij}$  and  $a$  that lead to low-energy virtual states in both channels. The corresponding cross sections  $\sigma_X$ ,  $\sigma_Y$ , and their sum are shown in Fig. 4 as functions of energy. The plot 4a corresponds to  $U_{XY} = 0$ , the plot 4b to  $U_{XY} = 20 \text{ MeV}$ , and the plot 4c to  $U_{XY} = -20 \text{ MeV}$ . In all three cases we use  $g_X = 1 \text{ fm}$  and  $g_Y = 0.3 \text{ fm}$ . For zero  $U_{XY}$ , there is no pronounced dip in the total cross section, as well as for  $U_{XY} = -20 \text{ MeV}$ . However, at  $U_{XY} = 20 \text{ MeV}$  the peaks in the cross section become more noticeable, and the cross section between peaks drops almost to zero. In the latter case there is also a dip in the cross section  $\sigma_X$  near the threshold of production of  $Y$ . Such a difference in the behavior of the cross sections is due to the interference of different terms in Eq. (13). Note that the cross sections are invariant under the simultaneous change of the signs of  $U_{XY}$  and  $g_Y$ .

Now we pass to the existence of a virtual state in the  $X$  channel and a low-energy bound state in the  $Y$  channel (see Fig. 5). For  $U_{XY} = 0$ , the bound state does not manifest itself, and the cross section  $\sigma_Y$  is small. However, when a small value of  $V_{XY}$  is introduced, the behavior of the cross section changes significantly. This is due to the transition of the bound state in the  $Y$  channel into the  $X$  channel with subsequent decay into  $B$  mesons. As a result, a resonant structure appears in the  $B\bar{B}$  production cross section.

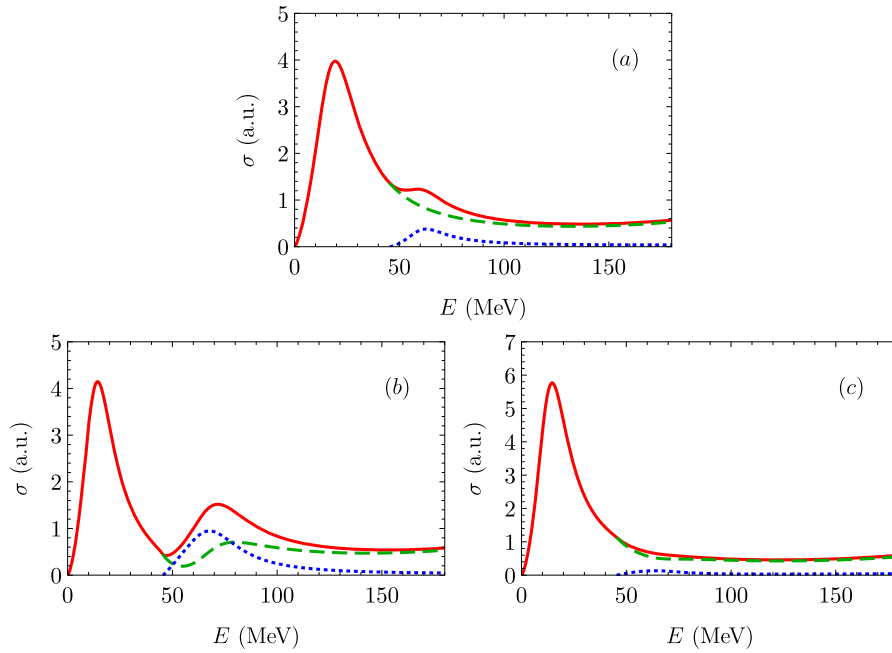


**Fig. 4.** The energy dependence of the cross sections  $\sigma_X$  (dashed line),  $\sigma_Y$  (dotted line) and their sum (solid line). The parameters of the model are  $U_{XX} = U_{YY} = -490$  MeV,  $a = 1.5$  fm,  $g_X = 1$  fm,  $g_Y = 0.3$  fm. On plot (a) off-diagonal potential  $U_{XY} = 0$ , on plot (b)  $U_{XY} = 20$  MeV, and on plot (c)  $U_{XY} = -20$  MeV.

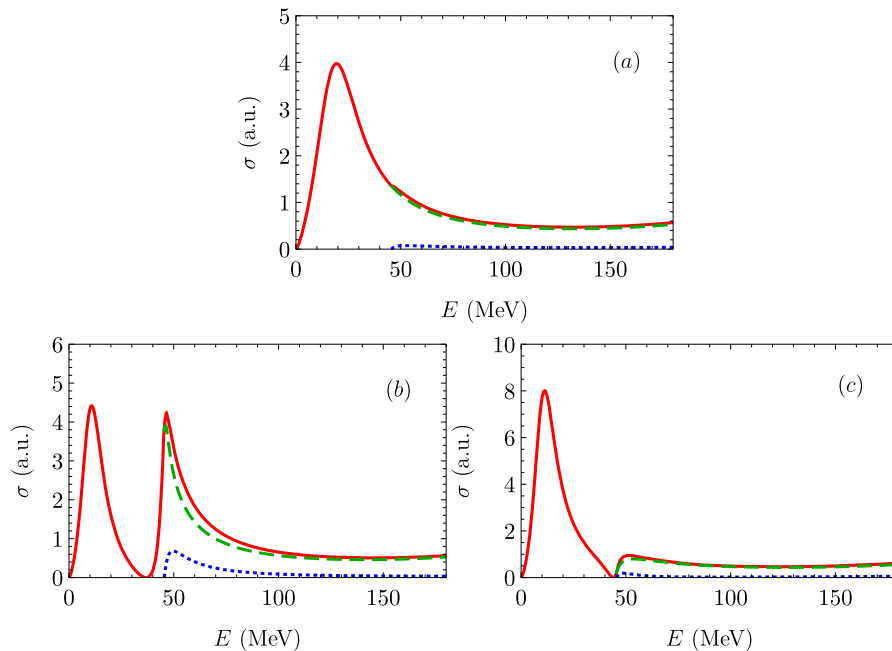


**Fig. 5.** The energy dependence of the cross sections  $\sigma_X$  (dashed line),  $\sigma_Y$  (dotted line) and their sum (solid line). The parameters of the model are  $U_{XX} = -490$  MeV,  $U_{YY} = -525$  MeV,  $a = 1.5$  fm,  $g_X = 1$  fm,  $g_Y = 0.3$  fm. On plot (a) off-diagonal potential  $U_{XY} = 0$ , on plot (b)  $U_{XY} = 20$  MeV, and on plot (c)  $U_{XY} = -20$  MeV.

For a low-energy bound state in the  $X$  channel and a virtual or a bound state in the  $Y$  channel, the energy dependence of the cross sections are shown in Figs. 6 and 7. In both cases there is no pronounced peak above the threshold of  $X$  state production. However, a peak above the threshold of  $Y$  state production can be seen in Fig. 6. This peak, corresponding to the virtual state, becomes more noticeable for one sign of  $U_{XY}$  and almost disappears for another sign. If there is a bound state in the  $Y$  channel, then there are no significant peaks in the cross section at  $U_{XY} = 0$ . However, for a small  $U_{XY}$ , a resonant structure manifests itself at the energy of a bound state. For one sign of the potential  $U_{XY}$ , there is a narrow and high peak in the cross section, and for another sign there is a sharp dip.

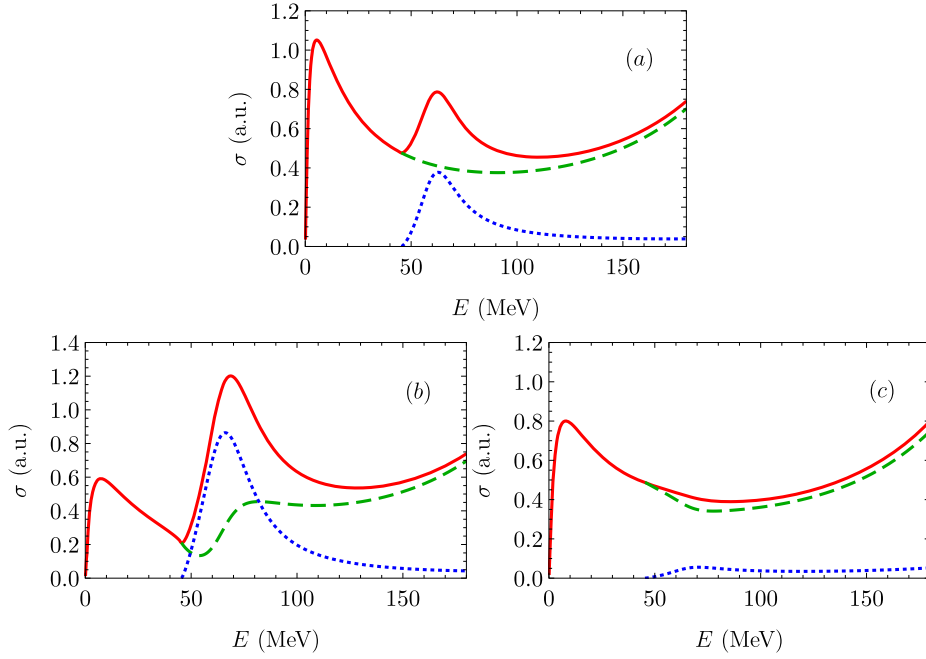


**Fig. 6.** The energy dependence of the cross sections  $\sigma_X$  (dashed line),  $\sigma_Y$  (dotted line) and their sum (solid line). The parameters of the model are  $U_{XX} = -525$  MeV,  $U_{YY} = -490$  MeV,  $a = 1.5$  fm,  $g_X = 1$  fm,  $g_Y = 0.3$  fm. On plot (a) off-diagonal potential  $U_{XY} = 0$ , on plot (b)  $U_{XY} = 20$  MeV, and on plot (c)  $U_{XY} = -20$  MeV.

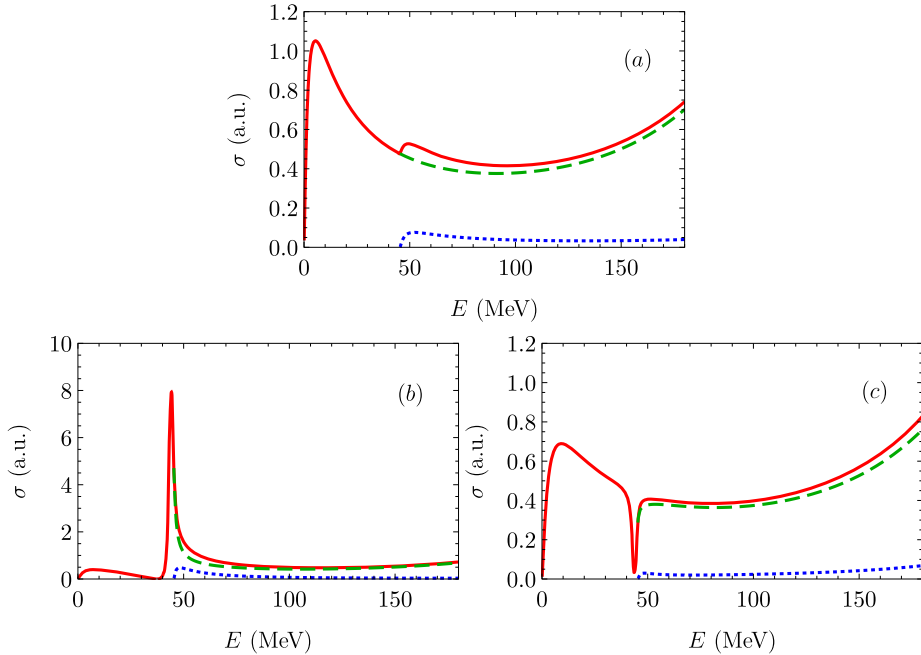


**Fig. 7.** The energy dependence of the cross sections  $\sigma_X$  (dashed line),  $\sigma_Y$  (dotted line) and their sum (solid line). The parameters of the model are  $U_{XX} = U_{YY} = -525$  MeV,  $a = 1.5$  fm,  $g_X = 1$  fm,  $g_Y = 0.3$  fm. On plot (a) off-diagonal potential  $U_{XY} = 0$ , on plot (b)  $U_{XY} = 20$  MeV, and on plot (c)  $U_{XY} = -20$  MeV.

Similar to one channels problem, we introduce the imaginary part of the optical potential. There are two elastic cross sections,  $\sigma_{el,X}$  and  $\sigma_{el,Y}$ , which are given by Eq. (13). There is also an inelastic cross section  $\sigma_{in}$  corresponding to the processes of annihilation of virtual  $X$  and  $Y$  states into other particles. The total cross section is a sum  $\sigma_{tot} = \sigma_{el,X} + \sigma_{el,Y} + \sigma_{in}$  and is expressed via the Green's function  $D(r, r'|E)$  of Eq. (12):

$$\sigma_{tot} = \frac{2\pi\alpha^2}{M_B s} \text{Im} [\mathcal{G}^\dagger D(0, 0|E) \mathcal{G}]. \quad (16)$$

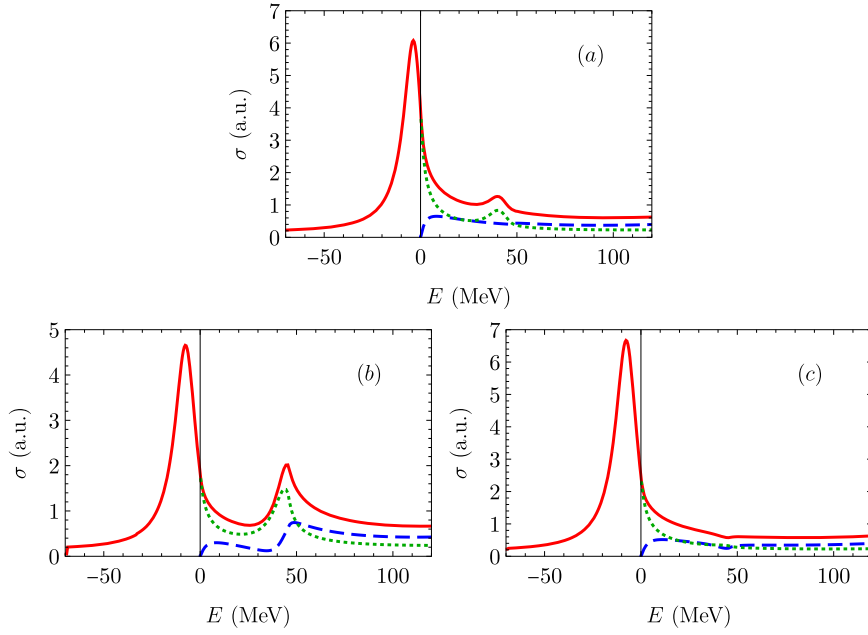


**Fig. 8.** The cross sections of hadron production for  $a = 1.5$  fm,  $U_{XX} = U_{YY} = (-525 - 10i)$  MeV,  $g_X = 1$  fm,  $g_Y = 0.3$  fm. On plot (a) off-diagonal potential  $U_{XY} = 0$ , on plot (b)  $U_{XY} = 20$  MeV, and on plot (c)  $U_{XY} = -20$  MeV. The dashed line corresponds to the elastic cross section, the dotted line to the inelastic cross section (annihilation into other mesons), and the solid line to the total cross section.

Here  $\mathcal{G} = (g_X, g_Y)^\dagger$ , and the superscript  $\dagger$  means the hermitian conjugation. In the two-channel case the Green's function is a matrix  $2 \times 2$  and satisfies the equation

$$\left( p_r^2 + M_B \mathcal{V} + \frac{l(l+1)}{r^2} - \mathcal{K}^2 \right) D(r, r' | E) = \frac{1}{rr'} \delta(r - r'). \quad (17)$$

The Green's function can be written in terms of the regular solutions  $\Psi_{1R}, \Psi_{2R}$  and the non-regular solutions  $\Psi_{1N}, \Psi_{2N}$  of Eq. (12):

$$\begin{aligned} D(r, r' | E) = & k_X (\Psi_{1R}(r) \Psi_{1N}^T(r') \theta(r' - r) + \Psi_{1R}(r') \Psi_{1N}^T(r) \theta(r - r')) \\ & + k_Y (\Psi_{2R}(r) \Psi_{2N}^T(r') \theta(r' - r) + \Psi_{2R}(r') \Psi_{2N}^T(r) \theta(r - r')). \end{aligned} \quad (18)$$

Corresponding upper ( $u_{1N}, u_{2N}$ ) and lower ( $v_{1N}, v_{2N}$ ) components of non-regular solutions of the Schrödinger equation have the asymptotics

$$\begin{aligned} u_{1N}(r \rightarrow \infty) &= \frac{1}{k_X r} \chi_X^+, & \lim_{r \rightarrow \infty} r v_{1N} &= 0, \\ \lim_{r \rightarrow \infty} r u_{2N} &= 0, & v_{2N}(r \rightarrow \infty) &= \frac{1}{k_Y r} \chi_Y^+. \end{aligned} \quad (19)$$

In all formulas of this subsection it is assumed that both  $k_X$  and  $k_Y$  have positive imaginary parts below the thresholds of the corresponding channels.

When both  $X$  and  $Y$  channels have low-energy bound states, the cross sections are shown in Fig. 8 for small values of  $\text{Im} V_{XX}$  and  $\text{Im} V_{YY}$ . For  $V_{XY} = 0$ , the bound states in both channels manifest itself only as peaks in the inelastic and total cross sections (see Fig. 8a). However, for  $V_{XY} = 20$  MeV, the bound state in the  $Y$  channel affects the elastic cross sections as well. As a result, the cross section  $\sigma_{\text{el},X}$  decreases below the threshold of  $Y$  state production, and the peak in the total cross section at energy near 50 MeV becomes more pronounced (see Fig. 8b). For another sign of the off-diagonal potential,  $V_{XY} = -20$  MeV, the interference between channels leads to the opposite effect. Namely, the peak in the cross section close to the threshold of  $Y$  state production disappears (see Fig. 8c).

### 2.3. Three channels

The most interesting case from the experimental point of view is the process in which the final state consists of hadron pairs in three channels with the same quantum numbers  $J^{PC} = 1^{--}$  but different spin states. To be specific, we consider the states  $X = B\bar{B}$ ,  $Y = (B^*\bar{B} - B\bar{B}^*)/\sqrt{2}$  and  $Z = B^*\bar{B}^*$ . As mentioned above, different spin of  $B$  and  $B^*$  mesons leads to slightly different interaction potentials in all three channels. The transitions between channels are possible, because the quantum numbers  $J^{PC}$  of all states are identical.

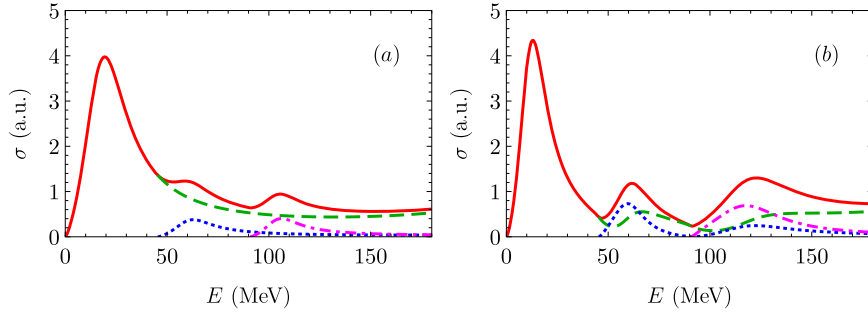


**Fig. 9.** The energy dependence of the cross sections  $\sigma_X$  (dashed line),  $\sigma_Y$  (dotted line),  $\sigma_Z$  (dash-dotted line) and their sum (solid line). The parameters of the model are  $U_{XX} = U_{YY} = U_{ZZ} = -490$  MeV,  $a = 1.5$  fm,  $g_X = 1$  fm,  $g_Y = 0.3$  fm,  $g_Z = 0.3$  fm. On plot (a) off-diagonal potentials  $U_{XY} = U_{XZ} = U_{YZ} = 0$ , on plot (b)  $U_{XY} = U_{XZ} = U_{YZ} = 20$  MeV.

The approach used for description of three-channel problem is a simple generalization of that for two-channel case. The corresponding Schrödinger equation reads

$$\left( p_r^2 + M_B \mathcal{V} + \frac{l(l+1)}{r^2} - \mathcal{K}^2 \right) \Psi(r) = 0, \quad \mathcal{K}^2 = \begin{pmatrix} k_X^2 & 0 & 0 \\ 0 & k_Y^2 & 0 \\ 0 & 0 & k_Z^2 \end{pmatrix}, \quad \mathcal{V} = \begin{pmatrix} V_{XX} & V_{XY} & V_{XZ} \\ V_{XY} & V_{YY} & V_{YZ} \\ V_{XZ} & V_{YZ} & V_{ZZ} \end{pmatrix}, \quad (20)$$

where  $k_Z = \sqrt{M_B(E - 2\Delta)}$ , and other momenta are defined in the previous subsection. In Eq. (20), the wave function  $\Psi = (u, v, w)^T$  consists of radial wave functions for the  $X$ ,  $Y$  and  $Z$  states. As above, the angular momentum of all states is  $l = 1$ .

The cross sections of pair production in each state are

$$\begin{aligned} \sigma_X &= \frac{2\pi\beta_X\alpha^2}{s} \left| g_X u_{1R}^{(1)}(0) + g_Y v_{1R}^{(1)}(0) + g_Z w_{1R}^{(1)}(0) \right|^2, \\ \sigma_Y &= \frac{2\pi\beta_Y\alpha^2}{s} \left| g_X u_{2R}^{(1)}(0) + g_Y v_{2R}^{(1)}(0) + g_Z w_{2R}^{(1)}(0) \right|^2, \\ \sigma_Z &= \frac{2\pi\beta_Z\alpha^2}{s} \left| g_X u_{3R}^{(1)}(0) + g_Y v_{3R}^{(1)}(0) + g_Z w_{3R}^{(1)}(0) \right|^2, \end{aligned} \quad (21)$$

where  $\beta_Z = k_Z/M_B$  and  $g_X, g_Y, g_Z$  are some constants related to the amplitudes of the corresponding state production at small distances. The functions  $u_{iR}, v_{iR}$  and  $w_{iR}$  are the components of three regular solutions  $\Psi_{iR}$ , having the asymptotics at  $r \rightarrow \infty$

$$\begin{aligned} \Psi_{1R} &= \frac{1}{2ik_X r} (S_{11}\chi_X^+ - \chi_X^-, S_{12}\chi_Y^+, S_{13}\chi_Z^+)^T, \\ \Psi_{2R} &= \frac{1}{2ik_Y r} (S_{21}\chi_X^+, S_{22}\chi_Y^+ - \chi_Y^-, S_{23}\chi_Z^+)^T, \\ \Psi_{3R} &= \frac{1}{2ik_Z r} (S_{31}\chi_X^+, S_{32}\chi_Y^+, S_{33}\chi_Z^+ - \chi_Z^-)^T, \\ \chi_X^\pm &= \exp[\pm i(k_X r - \pi/2)], \quad \chi_Y^\pm = \exp[\pm i(k_Y r - \pi/2)], \\ \chi_Z^\pm &= \exp[\pm i(k_Z r - \pi/2)], \end{aligned} \quad (22)$$

where  $S_{ij}$  are some coefficients.

In order to demonstrate how the transitions between channels affect the energy dependence of the cross sections, let us consider a few simple examples. We choose the parametrization of the potential in the form of rectangular wells with the same radius but different depths:

$$\mathcal{V} = \begin{pmatrix} U_{XX} & U_{XY} & U_{XZ} \\ U_{XY} & U_{YY} & U_{YZ} \\ U_{XZ} & U_{YZ} & U_{ZZ} \end{pmatrix} \theta(a - r), \quad (23)$$

where the matrix elements  $U_{ij}$  and the radius  $a$  are some constants. Below we present the numerical results obtained within this model for  $a = 1.5$  fm,  $g_X = 1$  fm,  $g_Y = 0.3$  fm,  $g_Z = 0.3$  fm, and various depths of the potential wells.

First consider the case when there are low-energy virtual states in all three channels. If the transitions between channels are absent, then the peaks corresponding to these virtual states are seen, but the contributions of the  $Y$  and  $Z$  states to the total cross section are small (see Fig. 9a). However, for the off-diagonal potentials  $U_{XY} = U_{XZ} = U_{YZ} = 20$  MeV, the peaks and dips in the cross sections are more pronounced (see Fig. 9b). Because of the transitions between channels, the cross section  $\sigma_X$  has strong energy dependence in the vicinity of  $Y$  and  $Z$  thresholds. Moreover, the cross section  $\sigma_Y$  becomes almost zero at the threshold of  $Z$  state. For the opposite signs of the mixing potentials the dips in the cross sections disappear and the peaks become less pronounced. If there

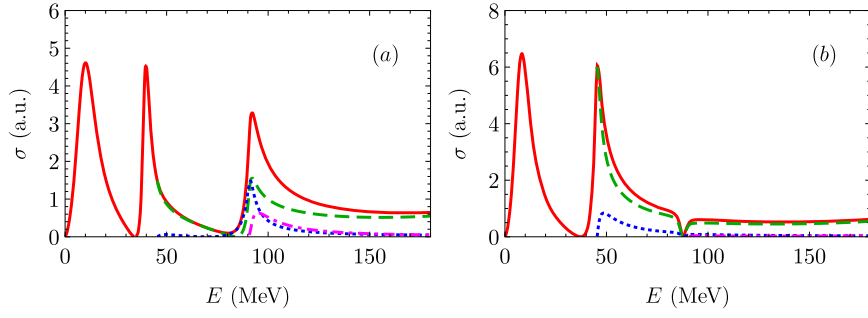


**Fig. 10.** The energy dependence of the cross sections  $\sigma_X$  (dashed line),  $\sigma_Y$  (dotted line),  $\sigma_Z$  (dash-dotted line) and their sum (solid line). The parameters of the model are  $U_{XX} = -490$  MeV,  $U_{YY} = U_{ZZ} = -525$  MeV,  $a = 1.5$  fm,  $g_X = 1$  fm,  $g_Y = 0.3$  fm,  $g_Z = 0.3$  fm. On plot (a) off-diagonal potentials  $U_{XY} = U_{XZ} = U_{YZ} = 20$  MeV, on plot (b)  $U_{XY} = 20$  MeV,  $U_{XZ} = -20$  MeV,  $U_{YZ} = 0$ .

are virtual states in each channel, then the energy dependence of the cross sections in the vicinity of each threshold looks similar to that for the two-channels problem, see Fig. 4.

Then consider a virtual state in the  $X$  channel and low-energy bound states in the other channels. If there are no transitions between channels, then these bound states are not observable. However, for  $U_{XY} = U_{XZ} = U_{YZ} = 20$  MeV, these states can decay into lighter particles. Namely, the bound state in the  $Y$  channel can pass into the  $X$  channel, and the bound state in the  $Z$  channel can pass into both  $X$  and  $Y$  channels. As a result, sharp peaks occur close to the thresholds of  $Y$  and  $Z$  states, and the total cross section falls almost to zero below these peaks (see Fig. 10a). Note that the energy dependence of the cross sections may change drastically for other values of mixing potentials. For instance, the cross section energy dependence for  $U_{XY} = 20$  MeV,  $U_{XZ} = -20$  MeV,  $U_{YZ} = 0$  is shown in Fig. 10b. The direct transition between the  $Y$  and  $Z$  channels is now forbidden, hence there is no pronounced peak corresponding to the bound state in the  $Z$  channel. Nevertheless, the total cross section has a sharp dip close to the threshold of the  $Z$  state production.

Obviously, other combinations of real and virtual states in the potentials, as well as the signs of the mixing potentials and the constants  $g_X$ ,  $g_Y$ ,  $g_Z$ , are also possible. For each set of parameters, the cross sections have their own peculiarities. We focused our attention on such parameters which lead to the energy dependence of the cross sections similar to the experimental one. The detailed description of the experimental data within our model is performed in the next section.

### 3. Production of $B^{(*)}\bar{B}^{(*)}$ near the thresholds

Precise measurement of  $B\bar{B}$ ,  $B\bar{B}^*$ ,  $B^*\bar{B}$ ,  $B^*\bar{B}^*$  pair production cross sections in  $e^+e^-$  annihilation near the thresholds of the corresponding processes [39,40], as well as the total cross section of these processes [21] demonstrate a non-trivial energy dependence. There are peaks with very unusual shape and deep dips in these cross sections (see Fig. 11). In this section, we show that our approach described above completely explains such a behavior.

As mentioned above, the states  $X = B\bar{B}$ ,  $Y = (B^*\bar{B} - B\bar{B}^*)/\sqrt{2}$  and  $Z = B^*\bar{B}^*$  have the same quantum numbers  $J^{PC} = 1^{--}$  and isospin  $I = 0$ . These quantum numbers correspond to the angular momentum  $l = 1$  of meson pairs. The spin of  $B^*\bar{B}^*$  pair can be  $S = 0$  or  $S = 2$ . At present, there is no experimental information on the contributions of specific spin states to the cross section of  $e^+e^- \rightarrow B^*\bar{B}^*$ . This is why, for simplicity, we consider both possible states as a single state. The thresholds of  $X$ ,  $Y$ , and  $Z$  channels are close to each other, so the transition amplitudes between these channels are essential.

The isotopic invariance violating effects, such as the Coulomb interaction between charged mesons and the mass difference of charged and neutral mesons, result in slight shift of peak positions in the cross sections of charged and neutral meson production. This effect has been studied in detail in Refs. [25,41]. Since the main goal of the present paper is to study the influence of transitions between several channels on the energy dependence of the cross sections, we do not discuss the effects of isotopic invariance violation. However, we have checked that these effects only slightly modify the energy dependence of the cross sections.

The exclusive cross sections of various final states ( $X$ ,  $Y$ , and  $Z$ ) production can be calculated directly by means of Eq. (21), where the wave functions are the corresponding solutions of the Schrödinger equation (20) for the three-channel case. For the description of experimental data, we use the parametrization of diagonal and off-diagonal potentials as the rectangular wells

$$V_{ij}(r) = U_{ij} \cdot \theta(a_{ij} - r), \quad i, j = X, Y, Z. \quad (24)$$

Of course, the model potentials (24) do not match the real interaction potentials. However, as explained above, if there are low-energy real or virtual states, the specific form of the potentials are not very important to reproduce the experimental data near the thresholds. The use of model potentials in the form (24) simplifies significantly calculation of the cross sections in the multichannel case.

Our analysis shows that it is possible to neglect the imaginary parts of  $U_{ij}$  since the probabilities for  $B^{(*)}\bar{B}^{(*)}$  pairs to annihilate into lighter particles are small. The quantities  $U_{ij}$ ,  $a_{ij}$ , as well as the complex constants  $g_X$ ,  $g_Y$ , and  $g_Z$ , are the seventeen fitting parameters of our model. The values of these parameters, which provide the best agreement of our predictions with the experimental data, are listed in Table 1. The corresponding value of  $\chi^2$  characterizing the agreement of predictions and experimental data is

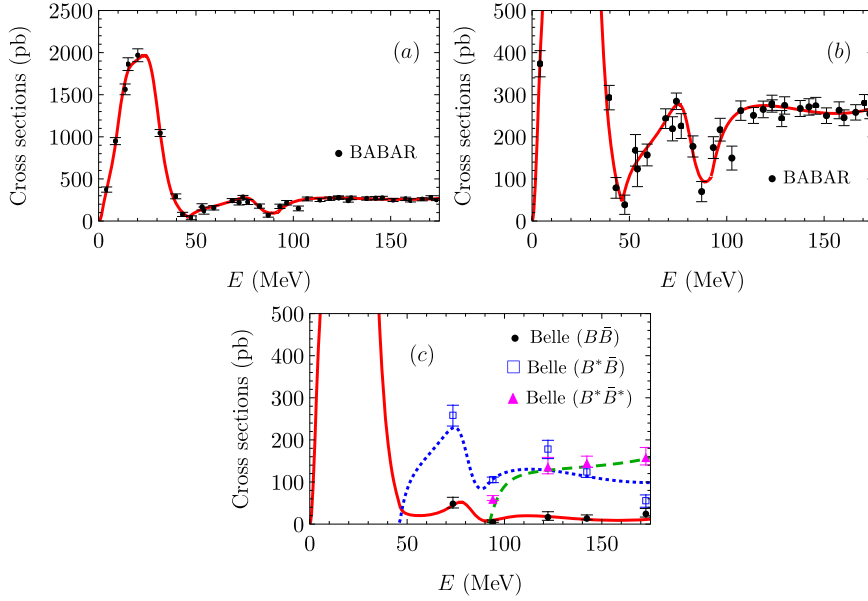


Fig. 11. The energy dependence of the cross sections of  $B$  mesons production. The total cross section  $\sigma_X + \sigma_Y + \sigma_Z$  is shown on plots (a) and (b) with the solid line. On plot (c) the exclusive cross sections  $\sigma_X$  (solid line),  $\sigma_Y$  (dotted line), and  $\sigma_Z$  (dashed line) are shown. Experimental data for the total cross section were recalculated in Ref. [38] using the data [21]. Experimental data for the exclusive cross sections are taken from Refs. [39,40].

**Table 1**  
Parameters of the model describing  $B$  mesons production in  $e^+e^-$  annihilation.

	$V_{XX}$	$V_{YY}$	$V_{ZZ}$	$V_{XY}$	$V_{XZ}$	$V_{YZ}$
$U_{ij}$ (MeV)	-613.1	-360.6	-586.7	26.7	20	78.6
$a_{ij}$ (fm)	1.361	1.804	1.809	0.953	2.819	2.209
$g_i$ (fm)	$g_X = 0.118$		$g_Y = -0.004 + 0.217i$		$g_Z = -0.6 + 0.193i$	

$\chi^2/N_{df} = 47/31 = 1.5$ , where  $N_{df}$  is the number of degrees of freedom. The energy dependence of the total cross section  $\sigma_{\text{tot}} = \sigma_X + \sigma_Y + \sigma_Z$ , as well as the exclusive cross sections  $\sigma_X$ ,  $\sigma_Y$ , and  $\sigma_Z$ , is shown in Fig. 11. Note that there are other sets of potential parameters that provide good agreement with experimental data. However, we rejected them for several reasons. Firstly, the values of the diagonal potentials differed from each other by several times. Secondly, the potential radii were either very small or very large compared to 1 fm. Thirdly, the off-diagonal potentials were very large. Under these restrictions, the potential parameters specified in the Table 1 are determined with an accuracy of a few percents. Similar to the case of two coupled channels discussed above, the energy dependence of the cross sections is invariant under the simultaneous change of signs of constants  $g_i$  and off-diagonal potentials. Therefore, only the relative signs of these quantities are important. In the Table 1 we present one of the possibilities.

In our work we consider the resonance structure of  $B^{(*)}\bar{B}^{(*)}$  production in  $e^+e^-$  annihilation near the threshold. This structure can be described either in terms of resonances in the quark-antiquark system, or in terms of resonances in the system of interacting  $B^{(*)}$ -mesons. For instance,  $Y(4S)$  meson can be considered as a  $b\bar{b}$  resonance and also as a resonance in  $B\bar{B}$  system. In this sense both approaches are equivalent, though the language of mesons and baryons is more convenient for qualitative predictions.

A peak in the total cross section corresponding to  $Y(4S)$  resonance is observed at an energy around 20 MeV. Within our model this peak is the result of the production of  $B\bar{B}$  pair near the threshold in the presence of a virtual state in this channel. There is also a peak at an energy around 75 MeV corresponding to  $B\bar{B}^*$  and  $B^*\bar{B}$  pair production, as well as a broad peak above 100 MeV associated with the production of  $B^*\bar{B}^*$  pairs. It turned out, however, that the positions and shapes of the latter two peaks depend strongly on the magnitude of the off-diagonal potentials responsible for the transitions between the channels. Although the magnitudes of these potentials are much smaller than the diagonal potentials (see Table 1), these magnitudes are comparable to the energies of real or virtual states, which are also small compared to the diagonal potentials. This is why the transitions between channels significantly affect the energy dependence of the cross sections. The transitions between channels are also responsible for the sharp dips in the cross section at energies near 45 MeV and 90 MeV. Neglecting the off-diagonal potentials, we obtain that the dips in the cross section practically disappear. It is seen that our model describes well the main features of the total cross sections.

Our model explains also the unusual energy dependence of the exclusive cross sections. For instance, there is a peak in  $\sigma_Y$  below the threshold of  $B^*\bar{B}^*$  production (see Fig. 11c). This peak is a manifestation of  $B^*\bar{B}^*$  bound state, because this state can decay into the  $Y$  channel. Thus, such a decay is possible solely due to the transitions between  $Y$  and  $Z$  channels. It is a very non-trivial effect, and its detailed study seems to be very important. Apparently, similar phenomena are also observed in the cross sections for the production of various  $D$  mesons, but this problem requires special investigation.

For zero off-diagonal potentials, the energy of  $B^* \bar{B}^*$  bound state is 67 MeV that is 25 MeV below the  $B^* \bar{B}^*$  threshold. We expect that this bound state can also manifest itself in the inelastic processes, where non- $B$ -meson final states are produced. The width of the peak in the corresponding cross sections is expected to be about 20 MeV.

#### 4. Conclusion

In our work, the production of hadron pairs near the thresholds is discussed, when there are low-energy bound or virtual states of produced particles. The consideration is based on the effective potential approach, which takes into account the interaction between hadrons in the final state. Particular attention is paid to the case when there are several reaction channels with nonzero transition amplitudes between them. It is shown that the energy dependence of the cross sections is very sensitive to the off-diagonal potentials, though the latter are small as compared to the diagonal ones. In particular, a narrow resonance below the threshold in one channel can lead to broad peaks in other channels.

Using our approach we have explained all available experimental data for the cross sections of  $B\bar{B}$ ,  $B^*\bar{B}$ ,  $B\bar{B}^*$  and  $B^*\bar{B}^*$  pair production in  $e^+e^-$  annihilation. It is shown that the non-trivial shape of the peaks in the cross sections, as well as the sharp dips, are the result of the transitions between different channels.

#### CRedit authorship contribution statement

All co-authors took equal parts in the investigation and writing original draft.

#### Declaration of competing interest

The authors declare that they have no known competing financial interests or personal relationships that could have appeared to influence the work reported in this paper.

#### Data availability

No data was used for the research described in the article.

#### References

- [1] V.F. Dmitriev, A.I. Milstein, Nucl. Phys. B - Proc. Suppl. 162 (2006) 53.
- [2] V.F. Dmitriev, A.I. Milstein, Phys. Lett. B 658 (2007) 13.
- [3] M. Goldberger, K. Watson, Collision Theory, Wiley, New York, 1964.
- [4] B. Aubert, et al., Phys. Rev. D 73 (2006) 012005.
- [5] J.P. Lees, et al., Phys. Rev. D 87 (2013) 092005.
- [6] R.R. Akhmetshin, et al., Phys. Lett. B 759 (2016) 634.
- [7] M. Ablikim, et al., Phys. Rev. Lett. 124 (2020) 042001.
- [8] M. Ablikim, et al., Phys. Lett. B 817 (2021) 136328.
- [9] R.R. Akhmetshin, et al., Phys. Lett. B 794 (2019) 64.
- [10] M. Ablikim, et al., Phys. Rev. D 91 (2015) 112004.
- [11] M. Ablikim, et al., Phys. Rev. D 99 (2019) 092002.
- [12] M.N. Achasov, et al., Phys. Rev. D 90 (2014) 112007.
- [13] M. Ablikim, et al., Nat. Phys. 17 (2021) 1200.
- [14] M.N. Achasov, et al., Eur. Phys. J. C 82 (2022) 761.
- [15] B. Aubert, et al., Phys. Rev. D 76 (2007) 092006.
- [16] M. Ablikim, et al., Phys. Rev. D 97 (2018) 032013.
- [17] M. Ablikim, et al., Phys. Rev. Lett. 123 (2019) 122003.
- [18] M. Ablikim, et al., Phys. Rev. D 107 (2023) 072005.
- [19] G. Pakhlova, et al., Phys. Rev. Lett. 101 (2008) 172001.
- [20] M. Ablikim, et al., Phys. Rev. Lett. 120 (2018) 132001.
- [21] B. Aubert, et al., Phys. Rev. Lett. 102 (2009) 012001.
- [22] J. Haidenbauer, X.-W. Kang, U.-G. Meißner, Nucl. Phys. A 929 (2014) 102.
- [23] J. Haidenbauer, U.-G. Meißner, Phys. Lett. B 761 (2016) 456.
- [24] J. Haidenbauer, U.-G. Meißner, L.-Y. Dai, Phys. Rev. D 103 (2021) 014028.
- [25] A.I. Milstein, S.G. Salnikov, Phys. Rev. D 104 (2021) 014007.
- [26] A.I. Milstein, S.G. Salnikov, Phys. Rev. D 105 (2022) 074002.
- [27] A.I. Milstein, S.G. Salnikov, Phys. Rev. D 105 (2022) L031501.
- [28] A.I. Milstein, S.G. Salnikov, Phys. Rev. D 106 (2022) 074012.
- [29] A.I. Milstein, S.G. Salnikov, Pisma v ZhETF 117 (2023) 901, JETP Lett. (2023).
- [30] B. Aubert, et al., Phys. Rev. D 73 (2006) 052003.
- [31] R.R. Akhmetshin, et al., Phys. Lett. B 723 (2013) 82.
- [32] P.A. Lukin, et al., Phys. At. Nucl. 78 (2015) 353.
- [33] B. Aubert, et al., Phys. Rev. D 71 (2005) 052001.
- [34] B. Aubert, et al., Phys. Rev. D 76 (2007) 012008.
- [35] M. Ablikim, et al., Phys. Rev. Lett. 117 (2016) 042002.
- [36] J. Haidenbauer, C. Hanhart, X.-W. Kang, U.-G. Meißner, Phys. Rev. D 92 (2015) 054032.
- [37] V.F. Dmitriev, A.I. Milstein, S.G. Salnikov, Phys. Rev. D 93 (2016) 034033.

- [38] X.-K. Dong, X.-H. Mo, P. Wang, C.-Z. Yuan, *Chin. Phys. C* 44 (2020) 083001.
- [39] R. Mizuk, et al., *J. High Energy Phys.* 2021 (2021) 137.
- [40] M. Bertemes, Quarkonium and charm physics at Belle II, in: *QCD & High Energy Interactions*, La Thuile, 2023.
- [41] A.E. Bondar, A.I. Milstein, R.V. Mizuk, S.G. Salnikov, *J. High Energy Phys.* 2022 (2022) 170.
- [42] S.M. Flatté, *Phys. Lett. B* 63 (1976) 224.